Morphological properties of Al-doped ZnO nano/microstructures

Kyung Ho Kim*, Tomoyuki Umakoshi, Yoshio Abe, Midori Kawamura, Takayuki Kiba

Department of Materials Science and Engineering, Kitami Institute of Technology, 165 Koen-cho, Kitami 090-8507, Hokkaido, Japan

Abstract

We discussed the morphological properties of Al-doped zinc oxide (Al-ZnO) microrods grown on a ZnO seed layer and precipitation particles and compared them with undoped ZnO samples. The ZnO nanorods grown on a ZnO seed layer were dense and perpendicular to the surface of the substrate, i.e., fluorine-doped tin oxide (FTO). In contrast the Al-ZnO grew as larger microrods, and the rods were sparsely and obliquely arranged. Precipitation particles synthesized in the ZnO solution through homogeneous nucleation had flower-like structures assembled from the rods and individual rods with lengths of several micrometers. Al-ZnO precipitation particles consisted of rods with length of several micrometers and hexagonal nanoplates. Fourier transform infrared (FTIR) analysis results showed that the rods and precipitation particles had the good chemical properties of ZnO. Both size and morphology of the rods could be effectively controlled by adding aluminum nitrate ($Al(NO_3)_3$) as dopant in the ZnO rod solution.

Keywords: ZnO; Al; Rods; Precipitation particles; pH

Corresponding author: Kyung Ho Kim (K.H. Kim)

Tel.: +81 157 26 9431; fax: +81 157 26 4973,

E-mail address: khkim@mail.kitami-it.ac.jp

1. Introduction

Zinc oxide (ZnO) nanostructures with various morphologies and sizes have attracted significant attention for fabrication of nanoscale electronic and optoelectronic devices [1-4]. The addition of dopants (Ga, In, Li, Cu, Al, etc) has been considered to be one of the easiest ways to control nanostructures produced by the wet chemical method [5-7]. For growth of the ZnO nanostructures on a seed layer-coated substrate, the dopant can be added in two ways: either in the seed layer solution or in the rods solution. In a previous study, we reported the structural properties of ZnO nanorods grown on the Al doped ZnO (Al-ZnO) seed layer and compared with those grown on the undoped ZnO seed layer [8]. With adding Al in the seed layer solution, the length of the nanorods increased without morphological change. Meanwhile, with the addition of Al to the rod solution, microrods instead of nanorods were produced [9].

On the other hand, the synthesis of ZnO precipitation nanoparticles has been studied as a function of the pH of precursor solution [10,11]. Sambath et al reported that the length and diameter of rod-like structures decreased with an increase in pH from 5 to 6.8 [10]. Wahab et al reported that sheet/plate-like nanostructures were observed in the case of pH of 6-7 [11]. The morphologies of the nanoparticles strongly depend on the synthesis method and conditions.

In this study, we analyzed the morphological properties of the Al-ZnO nanostructures grown on the ZnO seed layer and compared them with undoped ZnO nanostructures, and the properties of the Al-ZnO and ZnO precipitation particles synthesized from aqueous solutions were discussed.

2. Experimental

The ZnO and Al-ZnO nano/microstructures were grown on the 35-nm-thick-ZnO seed layers prepared on the fluorine doped tin oxide (FTO) coated glass substrates. The details of the fabrication process are described in our previous study [6].

To prepare undoped ZnO rods sample, an aqueous solution of zinc nitrae hexahydrate ($Zn(NO_3)_2{\cdot}6H_2O$, 0.01 M) and hexamethylenetetramine (HMT, $C_6H_{12}N_4$, 0.01 M) was prepared. For Al-ZnO sample, aluminum nitrate nonahydrate ($Al(NO_3)_3{\cdot}9H_2O$, 1 mM), as dopant, was added in the solution. The seed layer-coated FTO substrates were immersed vertically in the rod solutions then heated in a dry oven at 90 ^oC and 6 h. Then, the samples were rinsed with deionized water and dried at 120 ^oC for 10 min in the air ambient. After reaction, white precipitation particles were collected from the bottom of the beakers and dried at 120 ^oC for 10 min.

The structural properties were investigated using X-ray diffraction (XRD, Bruker, D8ADVANCE) and field emission scanning electron microscopy (FESEM, JSM-6701F) attached with an energy dispersive spectrometer (EDS). Chemical bonds of rods and precipitation particles were identified using Fourier transform infrared (FTIR, JASCO, FT/IR-6100) spectroscopy in the region 350-4000 cm^{-1}. The pH value of the solution was measured using a pH meter (HORIBA, D-54) before and after reaction.

3. Results and discussion

Figure 1 shows the cross-sectional FESEM images of (a) ZnO nanorods and (b) Al-ZnO microrods grown on the ZnO seed layers prepared on the FTO-coated glass substrates [6,9,12]. From XRD patterns, shown Fig.S1 in the supporting information, the wurtzite hexagonal structure of ZnO (JCPDS card no.36-1451) with no other impurities was identified in the samples. As shown in Fig.1(a), the undoped ZnO nanorods are well aligned and exhibit preferred orientation. Also, they have a uniform width (Fig.S2(a)). FESEM images of the ZnO seed layer and bare FTO substrate are shown in the Fig.S3, and these show the ZnO seed layer was composed of nanocrystals with size of several tens of nanometers. It has been reported that the presence of the seed layer decreases the interface energy between ZnO crystal and the substrate leading to the growth of dense and well-aligned nanorods [13,14]. In contrast by doping with Al in the ZnO solution, microrods instead of nanorods are grown and they are randomly inclined on the surfaces, as shown in Fig.1(b). The surface of the microrod shows smooth (Fig.S2(b)). The Al amount in the microrod calculated by EDS analysis is ~1.0 at% (see Table S1). The surface density of the Al-ZnO microrods is quite low compared with that of the ZnO nanorods. This shows that addition of Al dopant is an easy way to control the density and morphology of the rods. The inset image in Fig.1(a) shows the seed layer between the nanorods and the FTO substrate. However, it is no longer found in the Al-ZnO microrods sample, as shown the inset image in Fig.1(b).

Figure 2 shows the pH values of the solution before and after reaction. The initial pH values of the ZnO solution and Al-ZnO solution are ~7.1 and ~5.5, respectively. At initial neutral conditions, the undoped ZnO nanorods grew uniformly on the ZnO seed layer. However, in the Al-ZnO solution, the seed layer was partially etched because of the weakly acidic condition [15,16]. This surface promoted the growth of the microrods because of fewer nucleation sites and less special completion between rods [16,17]. After reaction at 90 ºC for 6 h, the pH value similarly increases in a similar way, to ~7.3 and ~7.2 for the ZnO solution and Al-ZnO solution, respectively [9,12].

Figure 3(a) shows the top-view FESEM image of the ZnO precipitation particles obtained from the solution. It reveals a large amount of flower-like structures assembled from rods and individual rods. The rod length is several micrometer. In neutral conditions, at a high level of supersaturation, homogenous nucleation in the solution and heterogeneous nucleation on the seed layer surface could spontaneously occur [16,18]. The shape of the single rods did not change because of the lowest surface free energy of the ZnO polar planes [19]. Meanwhile, the precipitated rods was bigger than the rods grown on the seed layer. This is because the high density of heterogeneous nuclei on the seed layer hinders the growth of the large rods from each individual nuclei [16].

The Al-ZnO precipitation particles, shown in Fig.3(b), is composed of rods with length of several micrometers and hexagonal nanoplates with diameter of several hundred nanometers (Fig.S4). The nanoplates are only observed in the Al-ZnO sample. It might be because the anion AlO_2^-, which supplied by the $Al(NO_3)_3$, hinders the growth along the [0001] direction by the reaction with Zn^{2+}, preferring lateral growth rather than vertical growth [20]. It reveals a high content of Al in the nanoplates (Table S1). During reaction, the pH of the Al-ZnO solution turns from acid to neutral [9,21], leading to growth of rod-type precipitations. .

Adding $Al(NO_3)_3$ to the ZnO solution made the initial pH condition changed from neutral to acidic and led to low homogeneous nucleation in the solution [16,18]. It was conclusively found that the amount of precipitation particles in the Al-ZnO solution was significantly less than those from the ZnO solution. The nuclei on the seed layer through heterogeneous nucleation are also fewer than those in neutral undoped ZnO solution. Therefore, under acidic conditions, the Al-ZnO microrods preferentially grow on the substrate.

Figure 4 shows the FTIR spectra of (a) ZnO nanorods, (b) Al-ZnO microrods, (c) ZnO precipitation particles, and (d) Al-ZnO precipitation particles. The absorption bands from 2400 to 2500 cm^{-1} are assigned to the asymmetric-stretch mode of CO_2 and moisture absorbs with the range of 3600-3900 cm^{-1} and 1400-1800 cm^{-1} [22]. The absorption peak at around 380 cm^{-1}, 420 cm^{-1}, and 560 cm^{-1} clearly indicates the presence of Zn-O stretching bond [23,24], in the all samples. Moreover, the O-H stretching bond at around 3500 cm^{-1}, C-O stretching bond at around 1360 cm^{-1}, and Al-O bond around 700-890 cm^{-1} observe in the Al-ZnO precipitation particles [24,25]. This might be related to the presence of the nanoplates in the Al-ZnO particles.

4. Conclusions

The structural properties of the ZnO and Al-ZnO nano/microstructures grown on the undoped ZnO seed layers-coated FTO substrates were investigated. The pH value of initial Al-ZnO rod solution was ~5.5, while, that of the ZnO rod solution was ~7.1. Well-aligned ZnO nanorods with a high density were grown on the ZnO seed layer. However, the randomly oriented Al-ZnO microrods with a low surface density were observed because of few nuclei sites, resulting from the partially etched seed layer. In the precipitation particles synthesized from the ZnO solution, flower-like structures composed of the rods and single rods with length of several micrometers were observed. In the Al-ZnO precipitation particles, we found both the micro-size rods and nanoplates. From FTIR analysis results, the formation of Zn-O was confirmed in the nano/microrods, ZnO and Al-ZnO precipitation particles. Thus, the Al dopant had a dramatic effect on the morphology and surface density of the ZnO nanostructures.

Figure captions

Figure 1. Cross-sectional FESEM images of (a) ZnO nanorods and (b) Al-ZnO microrods. Inset images are highly magnified images of the areas marked with dotted squares.

Figure 2. pH value of ZnO and Al-ZnO solutions: before (circle) and after (triangle) the reaction.

Figure 3. Top-view FESEM images of (a) ZnO and (b) Al-ZnO precipitation particles.

Figure 4. FTIR spectra of (a) ZnO nanorods, (b) Al-ZnO microrods, (c) ZnO precipitation particles, and (d) Al-ZnO precipitation particles.

References

[1] Z.L. Wang, Zinc oxide nanostructures: growth, properties and applications, J. Phys.: Condens. Matter. 16 (2004) R829-R858.

[2] F. Li, Y. Ding, P. Gao, X. Xin, Z.L. Wang, Single-crystal hexagonal disks and rings of ZnO: Low-temperature, large-scale synthesis and growth mechanism, Angew, Chem. Int. Ed. 43 (2004) 5238-5242.

[3] A.B. Djurišić, A.M.C. Ng, X.Y. Chen, ZnO nanostructures for optoelectronics: Materials properties and device applications, Prog. Quant. Electron. 34 (2010) 191-259.

[4] W.Y. Zhou, X.X. Zhang, D. Zhao, M. Gao, S.S. Xie, ZnO nanorods: morphology control, optical properties, and nanodevice applications, Sci. China Phys. Mech. Astron. 56 (2013) 2243-2265.

[5] S. Kim, G. Nam, H. Park, H. Yoon, S-h. Lee, J.S. Kim, J.S. Kim, D.Y. Kim, S-O. Kim, J-Y. Leem, Effects of doping with Al, Ga, and In on structural and optical properties of ZnO nanorods grown by hydrothermal method, Bull. Korean Chem. Soc. 34 (2013) 1205-1211.

[6] K.H. Kim, Z. Jin, Y. Abe, M. Kawamura, Effect of Li and Cu dopants on structural properties of zinc oxide nanorods, Superlattice. Microst. 77 (2015) 101-107.

[7] H-S. Hong, G-S. Chung, Controllable growth of oriented ZnO nanorods using

Ga-doped seed layers and surface acoustic wave humidity sensor, Sensor. Actuat. B 195 (2014) 446-451.

[8] T. Umakoshi, Y. Abe, M. Kawamura, K.H. Kim, Post-annealing effect of zinc oxide nanorods grown on Al-doped zinc oxide seed layers, Proc. IDW'14, pp.490-493 (2014).

[9] K.H. Kim, T. Umakoshi, Y. Abe, M. Kawamura, T. Kiba, Growth behavior of Al-doped zinc oxide microrods with times, Superlattice. Microst. 85 (2015) 743-746.

[10] K. Sambath, M. Saroja, M. Venkatachalam, K. Rajendran, N. Muthukumarasamy, Morphology controlled synthesis of ZnO nanostructures by varying pH, J. Mater. Sci: Mater. Electron 23 (2012) 431-436.

[11] R. Wahab, S.G. Ansari, Y.S. Kim, M. Song, H-S. Shin, The role of pH variation on the growth of zinc oxide nanostructures, Appl. Surf. Sci. 255 (2009) 4891-4896.

[12] K.H. Kim, T. Umakoshi, Y. Abe, M. Kawamura, T. Kiba, Determination of effective growth time for zinc oxide nanorods using chemical solution deposition, Superlattice. Microst. 88 (2015) 150-153.

[13] L. Vayssieres, K. Keis, S-E. Lindquist, A. Hagfeldt, Purpose-built anisotropic metal oxide material: 3D highly oriented microrod array of ZnO, J. Phys. Chem. B 105 (2001) 3350-3352.

[14] K. Yuan, X. Yin, J. Li, J. Wu, Y. Wang, F. Huang, Preparation and DSC application

of the size-tuned ZnO nanoarrays, J. Alloys Compd. 489 (2010) 694-699.

[15] X. Yan, Z. Li, R. Chen, W. Gao, Template growth of ZnO nanorods and microrods with controllable densities, Cryst. Growth Des. 8 (2008) 2406-2410.

[16] Y. Liu, W. Gao, Growth process, crystal size and alignment of ZnO nanorods synthesized under neutral and acid conditions, J. Alloys Compd. 629 (2015) 84-91.

[17] L.L. Yang, Q.X. Zhao, M. Willander, Size-controlled growth of well-aligned ZnO nanorod arrays with two-step chemical bath deposition method, J. Alloys Compd. 469 (2009) 623-629.

[18] T. Ichikawa, S. Shiratori, Fabrication and evaluation of ZnO nanorods by liquid-phase deposition, Inorg. Chem. 50 (2011) 999-1004.

[19] N. Fujimura, T. Nishihara, S. Goto, J. Xu, T. Ito, Control of preferred orientation for ZnOx films: control of self-texture, J. Cryst. Growth 130 (1993) 269-279.

[20] H. Huang, H. Wang, B. Li, X. Mo, H. Long, Y. Li, H. Zhang, D. Carroll, G. Fang, Seedless synthesis of layered ZnO nanowall networks on Al substrate for white light electroluminescence, Nanotechnology, 24 (2013) 315203-315209.

[21] J.Li, S. Srinivasan, G.N. He, J.Y. Kang, S.T. Wu, F.A. Ponce, Synthesis and luminescence properties of ZnO nanostructures produced by the sol-gel method, J. Cryst. Growth 310 (2008) 599-603.

[22] L.A. Chuprov, P.G. Sennikov, K.G. Tokhadze, S.K. Ignatov, O. Schrems, High-resolution fourier-transform IR spectroscopic determination of impurities in silicon tetrafluoride and silane prepared from it, Inorg. Mater. 42 (2006) 924-931.

[23] N. Xu, Y. Cui, Z. Hu, W. Yu, J. Sun, N. Xu, J. Wu, Photoluminescence and low-threshold lasing of ZnO nanorod arrays, Optics Express 20 (2012) 14857-14863.

[24] R. Wahab, Y-S. Kim, H-S. Shin, Fabrication, characterization and growth mechanism of heterostructured zinc oxide nanostructures via solution method, Curr. Appl. Phys. 11 (2011) 334-340.

[25] T. Ivanova, A. Harizanova, T. Koutzarova, B. Vertruyen, Optical characterization of sol-gel ZnO:Al thin films, Superlattice. Microst. 85 (2015) 101-111.

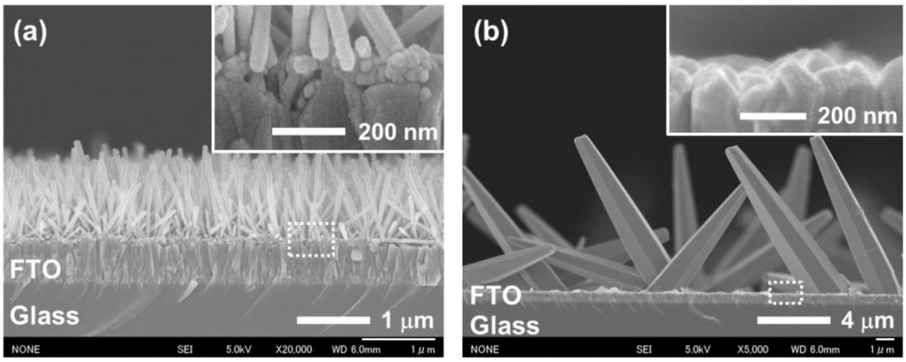
(a)
200 nm
FTO
Glass
1 μm
NONE SEI 5.0kV X20,000 WD 6.0mm 1 μm
(b)
200 nm
FTO
Glass
4 μm
NONE SEI 5.0kV X5,000 WD 6.0mm 1 μm

Figure 1

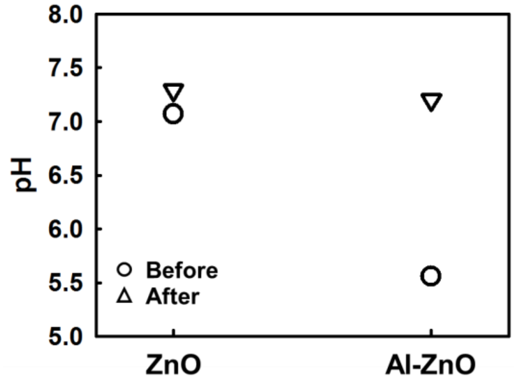

Figure 2

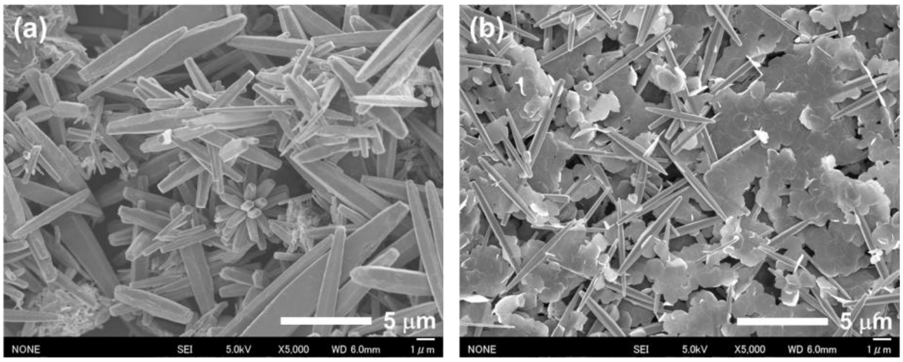
(a)
5 μm
NONE SEI 5.0kV X5,000 WD 6.0mm 1 μm
(b)
5 μm
NONE SEI 5.0kV X5,000 WD 6.0mm 1 μm

Figure 3

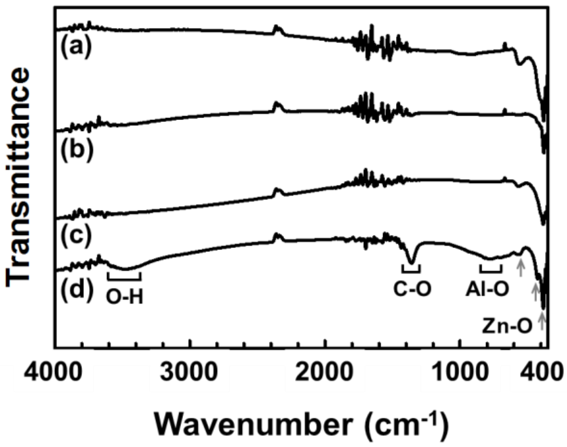
Transmittance
(a)
(b)
(c)
(d)
O-H
C-O
Al-O
Zn-O
4000
3000
2000
1000
400
Wavenumber (cm-1)

Figure 4